

G. J. Phillips

N 341 75-10

This material has been copied
under licence from CANCOPY.
Resale or further copying of this material is
strictly prohibited.

Paper Presented
at ANS 21st Annual Meeting
in New Orleans, 1975

Le présent document a été reproduit
avec l'autorisation de CANCOPY.
La revente ou la reproduction ultérieure
en sont strictement interdites.

HEAVY-WATER CRITICAL EXPERIMENT
FOR FUGEN (III)
CONTROL ROD EFFECTS

June, 1975

Mitsuo Matsumoto
Tohru Haga
Makoto Ueda

Power Reactor and Nuclear Fuel
Development Corporation, Japan.

A b s t r a c t

The control rod experiment has been done in Deuterium Critical Assembly (DCA) by using annular absorbers which simulate control rods of FUGEN reactor, a prototype heavy-water moderated, boiling-light-water cooled, and pressure tube type reactor. The DCA cores for this experiment use 1.2% enriched UO_2 fuel, and consist of 28-pin fuel clusters arranged in a square array of 22.5 cm lattice pitch. The experiment has been carried out with various control rod geometries, and also with varying coolant void fraction.

Experimental results have been analyzed by the "Absorption Area Method", which was employed in the calculation of the FUGEN control rod design. The calculated reactivity worth agreed with the experiment within $\pm 10\%$. The calculation tended to somewhat over-estimate the reactivity worth for the non-voided core, and under-estimate for the voided core. This tendency was greatly improved by considering the anisotropy effect of migration area M^2 of the cluster lattice.

C o n t e n t s

I	INTRODUCTION	1
II	EXPERIMENT	
	1. Outline of Experimental Facility	1
	2. Method of Reactivity Determination	2
	3. Critical Buckling, B_c^2	2
	4. Reactivity Coefficient of Water Level, $\partial\rho/\partial h$	4
	5. Results of Reactivity Measurement	5
	6. Flux Traverse	5
III	CALCULATION	
	1. Method of Calculation	6
	2. Linear Extrapolation Distance	7
	3. Absorption Area	8
	4. Reactivity Calculation	10
	5. Result of Calculation	10
IV	DISCUSSIONS	
	1. Variation of Control Rod Worth with Coolant Void Fraction	11
	2. Estimation of Anisotropy of Migration Area, M^2	12
V	CONCLUSIONS	13
VI	ACKNOWLEDGMENTS	14
VII	REFERENCE	14

I. INTRODUCTION

FUGEN is a heavy-water moderated, boiling-light-water cooled, and pressure tube type reactor. For reactivity control of this reactor, forty nine annular control rods are to be used, and the experimental investigation on these annular absorbers has been made by using DCA, a heavy water critical assembly.

For the design calculation of the control rod effect, a simple enough calculational technique is more desirable as long as it satisfies the required accuracy of the calculation. The method adopted in the design calculation of the FUGEN control rod is the "Absorption Area Method" (denoted hereafter by the A.A. Method).⁽¹⁾⁻⁽⁴⁾ The method was independently established for the FUGEN control rod analyses, but it was later found equivalent to the one developed by P. Greebler⁽²⁾.

A series of critical experiments were performed, to study the reliability of the calculational technique, in a heavy-water moderated, pressure-tube type critical facility DCA (Deuterium Critical Assembly)⁽⁵⁾.

In this paper, the details on the control rod experiments are presented together with the calculational method.

II. EXPERIMENT

1. Outline of Experimental Facility

The cross-sectional view of an experimental annular control rod is first shown in Fig. 1. The absorber elements are made of stainless-steel tube 0.59 ± 0.02 mm thick and 3.58 ± 0.03 mm in inner diameter, and they contain B_4C with a theoretical density of $70 \pm 1\%$. The control rod consists of these absorber elements assembled in a double concentric cylinder of 82 mm in outer diameter.

The physics parameters and core layout of the critical assembly are given in TABLE I, and Figs. 2, 3, respectively. The cores used for the experiment are of the 1.2% enriched UO_2 lattices consisting of 28-pin clusters in square arrays with 22.5 cm pitch. The intermediate coolant voiding, i.e., 30%, 70% and 86.7% void conditions, was simulated by mixing H_2O , D_2O , and

H_3BO_3 with adjustment of nuclear parameters. The void ratio values in TABLE I were determined by using a lattice-design code METHUSELAH-II⁽⁶⁾⁻⁽⁸⁾, in such a way as to conserve the slowing-down power $\xi \Sigma_s$ of the void-simulated lattice.

The control rods were inserted in-between the fuel assemblies through the "experimental hole" (see Fig. 3). The maximum number of inserted absorber rods was 9.

2. Method of Reactivity Determination

Figure 4 shows the experimental procedure to determine the reactivity worth of the control rods. The reactivity worth of the control rods (abbreviated hereafter by CR-worth) is obtained by integrating the calibrated moderator level worth curve between two critical moderator levels with and without absorber rods in the core. Since the critical D_2O -moderator height is affected by the coolant level in the fuel channel, it is always adjusted to the condition when there is no level difference between them. The $\partial\rho/\partial h$ value was measured by the positive-period method. The effective delayed neutron fraction was evaluated by using delayed neutrons parameters⁽⁹⁾ for ^{235}U and ^{238}U , and photo-delayed neutron parameters⁽¹⁰⁾⁻⁽¹¹⁾ for deuterium. The $\partial\rho/\partial h$ value is affected slightly by the moderator-coolant level difference LD and also by the strength of neutron absorber CR. Both were considered in the measurements.

3. Critical Buckling, B_c^2

The reactivity loss due to the insertion of CR was compensated by increasing core height, i.e., by supplying D_2O -moderator into the core tank. Neither the operational control rod nor the liquid poison, etc. was used in this case. In most measurements, the LD-value was in the range $-15 \sim +15$ cm. This required correction of the observed critical moderator height in the range from $+1.0$ to -2.0 cm. The relationships between LD's and observed critical moderator heights were investigated experimentally, and were analyzed with one-dimensional diffusion calculation.

The reflector saving in the axial direction, i.e., δ -value, was obtained by the least square fit of the Cu wire activation to a sine function. A number of Cu wires were irradiated at the centers of fuel clusters and of moderator space. Activation data with 10cm from both the core boundaries (top and bottom) were excluded from the least square fitting to eliminate the non-asymptotic effect. Measurement showed that the δ -value in the fuel cluster (δ_F) was slightly larger than that in the moderator (δ_M), i.e., by about 1 ~ 3cm in the 0% and 30% voided lattice. Strictly speaking, this phenomenon indicates a difficulty of evaluating δ -values by homogeneous treatment. A simple method was employed here to obtain the average δ value for practical purpose. The cell-averaged reflector saving δ is then given by

$$\frac{1}{\delta} = \left\{ \frac{1}{\delta_F} + \frac{1}{\delta_M} \frac{(V\phi)_M}{(V\phi)_F} \right\} / \left\{ 1 + \frac{(V\phi)_M}{(V\phi)_F} \right\} \quad (1)$$

where $(V\phi)_M$ and $(V\phi)_F$ are the volume integral of the thermal flux in moderator and fuel channel. Also, it is assumed that the same vacuum boundary condition will hold for each medium.

Since the values of δ_F , δ_M , and δ were influenced by the moderator-coolant level difference LD, the measured δ_F , δ_M , and δ were always corrected to the LD = 0 condition, and the results are shown in Table II. Experimental uncertainty of δ values was estimated to be within ± 0.5 cm. The uncertainty resulting from the application of Eq. (1) was not considered. It was also found that the values of δ_F and δ_M were insensitive whether the CR's exist or not.

The radial buckling in the clean core was also determined from the Jo function least square fit of Cu wire activation irradiated both in the centers of fuel clusters and of moderator. The activation traverse in the moderator space resulted in the same radial buckling as that obtained in the fuel space. The measurements were done for 0% and 100% void cores, and the value was $2.40 \pm 0.05 \text{m}^{-2}$ for both

cases. Hence, the radial buckling in the clean core was assumed independent of coolant void ratio.

4. Reactivity Coefficient of Water Level,
 Reactivity coefficient of water level $\frac{\partial \rho}{\partial h}$ is,

$$\frac{\partial \rho}{\partial h} = \frac{1}{\beta_{\text{eff}}} \frac{1}{k_{\text{eff}}^2} \frac{\partial k_{\text{eff}}}{\partial h} \quad (2)$$

The reactivity changes from ρ^A to ρ^0 due to withdrawal of CR, and the negative CR-worth at the core height h is given by,

$$\begin{aligned} \rho(h) &= \rho^0 - \rho^A \\ &= \int_{h_c^0}^h \left(\frac{\partial \rho}{\partial h}\right)^0 dh - \int_{h_c^A}^h \left(\frac{\partial \rho}{\partial h}\right)^A dh \\ &= \int_{h_c^0}^{h_c^A} \left(\frac{\partial \rho}{\partial h}\right)^0 dh - \int_{h_c^A}^h \left\{ \left(\frac{\partial \rho}{\partial h}\right)^A - \left(\frac{\partial \rho}{\partial h}\right)^0 \right\} dh \\ &= \rho(h_c^A) - \int_{h_c^A}^h \left\{ \left(\frac{\partial \rho}{\partial h}\right)^A - \left(\frac{\partial \rho}{\partial h}\right)^0 \right\} dh, \quad (3) \end{aligned}$$

where $\left(\frac{\partial \rho}{\partial h}\right)^0$ and $\left(\frac{\partial \rho}{\partial h}\right)^A$ are reactivity coefficient of water level without and with CR respectively, h_c^0 is the critical moderator height without CR and h_c^A with CR.

If the axial buckling is given by $\pi^2/(h + \delta)^2$, one-group treatment of $\partial \rho / \partial h$ becomes,

$$\frac{\partial \rho}{\partial h} = \frac{2 \pi M_z^2}{\beta_{\text{eff}} k_{\infty}} \cdot \frac{1}{(h + \delta)^3} \equiv \frac{a}{(h + \delta)^3}, \quad (4)$$

where M_z^2 is the migration area in the axial direction, and the coefficient a is called hereafter as "a-value". The a-value is generally known to be almost a constant in water moderated system.

Behavior of $\partial \rho / \partial h$ with CR insertion was also studied numerically by a few-group diffusion calculation. Two-group,

two-dimensional diffusion calculation was performed, and the core averaged values of M^2 and K_∞ were obtained with CR's in the core. It was found that the M^2/K_∞ was linearly related to the critical axial buckling $B_z^2 (h_c^A)$, and that the ratio was insensitive to the position of CR insertion. Reactivity $\Delta\rho$ of level increment from the critical height h_c to $h_c + \Delta h$ yields the ratio $\Delta\rho/\Delta h$ at a level of $h_c + \Delta h/2$. The a-value was then given by,

$$a = \left(\frac{\Delta\rho}{\Delta h} \right) (h_c + \Delta h/2 + \delta)^3 \quad (5)$$

The a-values at various critical core heights obtained in this manner were fitted to a linear function with respect to $B_z^2 (h_c)$. Since the possible $\Delta\rho$ in the experiment is limited within ~ 20 cents at most, the Δh increment is only in the range $0.2 \sim 1.0$ cm. This limitation caused in the worst case more than $\pm 3\%$ of uncertainty in the evaluated individual a-values, which happened in the clean critical core. The result of the least square fit would give more accurate a-values with the uncertainty of about $\pm 1.5\%$.

5. Results of Reactivity Measurement

The axial critical bucklings $B_z^2 (h_c^A)$ together with the CR-worths ρ at fixed buckling, $B_z^2 = 6.11 \text{ m}^{-2}$, are given in TABLE III. The CR-worths ρ at an arbitrary buckling B_z^2 can be derived by using Eqs.(3), (4), and the a-values of TABLE II. Experimental uncertainty in $B_z^2 (h_c^A)$ is about $\pm 0.07 \text{ m}^{-2}$, and relative errors of reactivity measurements vary around $2.0 \sim 2.5\%$ depending on the void conditions.

Single-annulus CR-worths were measured at the position 1C1 (see Fig.3) in the non-voided core. The individual worths for the inner- and outer- annuli were smaller by 16% and 2%, respectively, as compared with the worth of normal double annulus.

6. Flux Traverse

For cores having a multiple number of CR's, activation traverses were made by irradiating Cu wires at the centers in the fuel clusters. Since the irradiation was done without any filters, these measurements include the effect of the epithermal neutrons. However, the relative activation shapes may be regarded as those by pure thermal neutrons

within experimental accuracy, because the cadmium ratio of the Cu wire activity is around 20. The results of these flux traverses are shown in TABLE IV.

III CALCULATION

1. Method of Calculation

The design calculation of the FUGEN CR's is based on the "Absorption Area Method" (A.A. method)⁽²⁾. Interference effect of multiple CR's is taken into the "absorption areas" by adopting the "controlled super-cell" model. The direct full-core diffusion calculation applying the logarithmic derivative condition on the surface of CR (L.D. method) requires much computer time when multiple CR's are inserted in various rod-patterns. The L.D. method may be useful, however, as an alternative since it reproduces better flux shape near the CR's. The procedure of calculations is shown in the flow chart of Fig. 5. Three-group cell constants were obtained by the METHUSELAH-II code. It generates fluxes, reaction rates, group constants, multiplication factors, etc. of a cluster lattice in five energy groups (three fast and two overlapping thermal groups), and also in two groups (one fast and one thermal groups).

In the CR analysis, three-group approximation are employed. "Fast group" is the collapse from fast two-groups, i.e., 10 MeV - 5.53 KeV, and epithermal group corresponds to the third group of the METHUSELAH-II code.

It is assumed that the CR is transparent to the fast neutron, and the CR absorbs epithermal and thermal neutrons only. A controlled super-cell model is considered to obtain the linear extrapolation distances on the surface of the CR. As shown in Fig.6, the super-cell consists of four fuel assemblies with a CR in their center. The super-cell is then cylindricalized to make transport calculations in one dimensional geometry. To make homogenization in each annulus region, the atomic number density was adjusted in such a way as to conserve the effective reaction rate considering the fine structure of thermal neutron flux distribution. In these transport calculations, THERMOS code is used for thermal flux, and DTF code for epithermal flux.

In the case of a direct full core diffusion calculation in X-Y coordinate by L.D. method, the cylindrical CR's have to be changed to the effectively equivalent square rods. To do this, H. Hurwitz's proposal ⁽¹⁾ was employed, and the square CR of 6.95cm width was determined.

2. Linear Extrapolation Distance

The linear extrapolation distance for the thermal neutrons (d_3) is estimated from the thermal flux distribution and absorption rate around the CR. The total neutron absorption ($(S\phi)_3$) in the CR annulus is equal to the integral neutron current into the outer and inner surface of the annulus. Assuming that the linear extrapolation distance into the CR annulus is equal on the both surfaces, d_3 is given by

$$d_3 = \frac{\lambda_{tr,3}}{3\alpha_3} \left\{ (S\phi_3)_{out} + (S\phi_3)_{in} \right\}, \quad (6)$$

where $\lambda_{tr,3}$ is a transport mean free path near the surface of the annulus, and S_{out} and S_{in} are the area of the outer and inner surfaces, respectively.

The linear extrapolation distance for the epithermal neutrons (d_2) is evaluated by considering the epithermal flux distribution, absorption rate and slowing down rate around the CR's. The total epithermal neutron removal in the cylindrical CR ($(S\phi)_2$) is the sum of the absorbed epithermal neutrons and the slowed down loss to the thermal group, subtracting the slowed down gain from higher energy group. It is equal to the epithermal neutron into the CR. The linear extrapolation distance for epithermal neutrons (d_2) is then given by

$$d_2 = \frac{\lambda_{tr,2}}{3\alpha_2} (S\phi_2)_{out} \quad (7)$$

where $\lambda_{tr,2}$ is a transport mean free path of epithermal neutrons in the outer medium.

3 Absorption Area

Total number of slowing down neutrons in the super-cell is proportional to its area, and some fraction of slowed down neutrons is absorbed by the CR. The absorption area is therefore related to the total number of neutrons lost to the CR, and it is expressed in terms of the equivalent area of slowing down source neutrons.

For the i -th group neutrons, it is given by,

$$A_i \equiv \frac{\text{The } i\text{-th group absorption rate by a CR}}{\text{Slowing down density into the } i\text{-th group}} \\ = \frac{-2\pi r_0 J_i(r_0)}{\sum s_{i-1} \phi_{i-1}} \quad (8)$$

where r_0 is the radius of the CR and $-J_i(r_0)$ is the neutron current on the CR surface.

It is assumed that;

- (1) the fast neutrons are not absorbed by the CR and the slowing down source distribution to the epithermal group is flat, and
- (2) the flux is the function of radial distance (r) only in the super-cell calculation.

Then, epithermal and thermal fluxes obey,

$$\nabla^2 \phi_2 - \frac{1}{L_2^2} \phi_2 + \frac{Q}{D_2} = 0, \quad (9)$$

$$\nabla^2 \phi_3 - \frac{1}{L_3^2} \phi_3 + \frac{\sum s_{1,2}}{D_3} \phi_2 = 0, \quad (10)$$

where L_2, L_3 are the diffusion length for epithermal and thermal neutrons; D_2, D_3 are the diffusion constants; $\sum s_{1,2}$ is the slowing down cross section from epithermal group; and Q is the fast neutron slowing down source. The boundary conditions applied for these equations are;

Q is spatially independent

- (1) the logarithmic derivative boundary condition on the CR surface, and
 (2) the flat boundary condition at the end of the super-cell.
 The second boundary condition expresses the shadowing effect of the adjacent CR's spaced uniformly.

Obtaining the epithermal and thermal flux distributions from Eq. (9)~(10), the absorption areas for each group of neutrons are given by,

$$A_2 = \frac{2\pi r_0 L_2}{\alpha(2) + d_2/L_2} \quad (11)$$

$$A_3 = \frac{2\pi r_0 L_3}{\epsilon} \left[\frac{1}{\frac{L_2}{L_3}(1-L_3^2/L_2^2)} \times \frac{1}{\alpha(2) + \frac{d_2}{L_2}} + \zeta \frac{1}{\alpha(3) + \frac{d_3}{L_3}} \right] \quad (12)$$

where $\epsilon = 1 - \frac{\alpha'(2)}{\alpha(2) + \frac{d_2}{L_2}}$, (13)

$$\zeta = 1 - \frac{1}{1-L_3^2/L_2^2} \times \frac{\alpha(2) + \frac{d_3}{L_2}}{\alpha(2) + \frac{d_2}{L_2}} \quad (14)$$

$$\alpha(i) = \frac{I_1(R_0/L_i)K_0(r_0/L_i) + K_1(R_0/L_i)I_0(r_0/L_i)}{I_1(R_0/L_i)K_1(r_0/L_i) - K_1(R_0/L_i)I_1(r_0/L_i)} \quad (15)$$

$$\alpha'(2) = \frac{I_1(R_0/L_2)K_0(R_0/L_2) + K_1(R_0/L_2)I_0(R_0/L_2)}{I_1(R_0/L_2)K_1(r_0/L_2) - K_1(R_0/L_2)I_1(r_0/L_2)} \quad (16)$$

and I_0 , I_1 , K_0 and K_1 are the Bessel functions.

The shadowing of the adjacent CR's influences the absorption areas, and this shadowing effect is shown in Fig.7 taking an example in the non-voided core, where $A_2(\infty)$ and $A_3(\infty)$ are the absorption areas having no shadowing effect. In DCA experiment, R_0/L_2 and R_0/L_3 vary in the range 2.7 ~ 3.9, 2.7 ~ 3.9,

respectively, with changing void conditions. Therefore, the shadowing loss of absorption areas is expected about 2% maximum.

4. Reactivity Calculation

Introducing the concept of the absorption area, the three group diffusion equations in the reactor obey,

$$- D_1 \nabla^2 \phi_1 + \Sigma_{s1,1} \phi_1 + \Sigma_{a,1} \phi_1 = \nu \Sigma_{f,1} \phi_1 + \nu \Sigma_{f,2} \phi_2 + \nu \Sigma_{f,3} \phi_3, \quad (17)$$

$$- D_2 \nabla^2 \phi_2 + \Sigma_{s1,2} \phi_2 + \Sigma_{a,2} \phi_2 = F_2 \Sigma_{s1,1} \phi_1, \quad (18)$$

$$- D_3 \nabla^2 \phi_3 + \Sigma_{a,3} \phi_3 = F_3 \Sigma_{s1,2} \phi_2, \quad (19)$$

$$\text{where } F_i = \frac{A_c - A_i}{A_c}. \quad (20)$$

The factor F_i indicates the rate of i -th group source neutron reduction due to the CR in the considered super-cell. If the flux distribution is represented using local buckling, the reduced fission cross sections also give the correct multiplication factor, i.e.,

$$\nu \Sigma_{f,2} \rightarrow F_2 \nu \Sigma_{f,2}, \quad (21)$$

$$\nu \Sigma_{f,3} \rightarrow F_2 F_3 \nu \Sigma_{f,3}. \quad (22)$$

In the present analysis, this reduced fission source is mostly used for the controlled super-cell.

5. Result of Calculation

The calculated results are shown in TABLE V as compared with the experiments. The calculations of reactivity worths using the A.A. method agreed with the experiments within about $\pm 10\%$. For the design calculation, the A.A. method is simple and effective enough to know the CR effects.

When non-voided and voided core were compared, it was predicted that the CR worths increase for the voided core. Physically, it is understood that the result is attributed to the large neutron diffusion area of the voided core.

An example of the calculated thermal flux distribution with 9 control rods in the non-voided core (core No.23) is shown in Fig.8 together with the measurements. The agreement between the experiment and calculation was found reasonably good. The direct whole-core diffusion calculation with the logarithmic derivative boundary conditions on the rod surface (L.D. Method) was found better to predict the flux distribution, although it required much more computer time.

IV. DISCUSSION

1. Variation of Control Rod Worth with Coolant Void Fraction

In TABLE III, it is shown that the CR worth increases with increasing coolant void fraction. Consequently, the coolant void dependence of CR worth may be interpreted by a two-group CR theory by A.M. Weinberg et al. (12)

With a slight reformation of the formula given in Ref. (12), the central control rod worth is given by,

$$\rho = \frac{a}{2\pi^2} \Delta B_z^2, \quad (23)$$

$$a \equiv \frac{2\pi^2 M_z^2}{\beta_{eff} k_{\infty}}, \quad (24)$$

$$\Delta B_z^2 = \left(\frac{7.45}{R} \right) \cdot \left[0.116 \left(1 + \frac{\tau}{L^2} \right) + \frac{\tau}{L^2} \ell_n \left(\frac{L\sqrt{\tau}}{M^2 R_{eff}} \right) + \ell_n \left(\frac{R}{2.405 R_{eff}} \right) \right]^{-1}, \quad (25)$$

where R is the effective core radius, 155cm in DCA core, R_{eff} is the effective radius of CR, 3.5cm in the present study. The CR is

assumed to be black to thermal neutrons, but transparent to the fast ones. The isotropic τ - and L^2 -values in Eq. (25) were obtained from METHUSELAH-II code : τ -values; 94, 104, 123, 134, and 180cm², and L^2 -values; 70, 74, 82, 85 and 83cm², for the cores of 0, 30, 70, 86.7 and 100% voids, respectively. Numerical study showed that the experimental a-value, including anisotropy of M^2 , reproduced the void dependence of CR worth very well, but the calculated a-value, neglecting the anisotropy of M^2 , did not. Equation (23) over-estimated the CR-value by about 20% in the 100% voided core, for which the isotropic effect of M^2 being considered.

2. Estimation of Anisotropy of Migration Area, M^2

As discussed in the preceding section, the anisotropy of M^2 may play an important role of the CR-worth. In a simple 2-group approximation, the a-value is given by,

$$a = \frac{2\pi^2 M^2}{\beta_{\text{eff}} k_{\infty,2}^*} \left(1 + 2 \frac{\tau L^2}{M^2} B_c^2 \right), \quad (26)$$

where τL^2 and M^2 are isotropic values, and $k_{\infty,2}^*$ is the "two-group multiplication factor in a finite reactor", distinguished from k_{∞} by C.R. Richey et al.⁽¹³⁾ and by Ueda.⁽¹⁴⁾ The $k_{\infty,2}^*$ is expressed by the two-group constants which are defined in a finite reactor as follows:

$$k_{\infty,2}^* = \left(\frac{\nu \Sigma_f}{\Sigma_a} \right)_T \left(\frac{\Sigma_{sd}}{\Sigma_{sd} + \Sigma_a} \right)_F \left\{ 1 + \frac{(\nu \Sigma_f)_F}{(\nu \Sigma_f)_T} \frac{\Sigma_a T}{\Sigma_{sd} F} (1 + L^2 B^2) \right\}, \quad (27)$$

and is related to k_{eff} by the well-known "form"

$$k_{\text{eff}} = k_{\infty,2}^* / \left\{ (1 + \tau B^2)(1 + L^2 B^2) \right\} \quad (28)$$

The suffixes F and T refer to fast and thermal neutron groups. The value of $k_{\infty,2}^*$ is larger than k_{∞} by about 1 ~ 2% in the present lattices. The values of $k_{\infty,2}^*$ and M^2 (isotropic) were experimentally determined by M Ueda.⁽¹⁴⁾ The ratio M^2/M^2 can be calculated from

Eq. (26). The values of M_z^2/M^2 obtained in this manner are 0.95, 0.88, 0.99, 1.18, and 1.16 for the cores of 0, 30, 70, 86.7, and 100% voids, respectively. The isotropic value of M^2 is expected to have uncertainty of about $\pm 6\%$, and it results in about $\pm 1.5 \sim 2\%$ of relative error in the a -values. Also, the value of β_{eff} might have some systematic uncertainties, and the M_z^2/M^2 evaluated in this way may not yet well refined for precise study of migration-isotropy. The M_z^2/M^2 value, however, is useful to interpret the difference of CR-worth between experiment and calculation.

V. CONCLUSION

A series of control rod experiments were performed in a heavy-water moderated, pressure-tube type critical facility, DCA, to study the physics of the annular control rods (CR's) to be used in the FUGEN reactor. Reactivity worths of the CR's were determined from the difference of the critical core heights with and without the CR's. Flux traverse measurements were made in various core configurations. The experiment was carried out by changing the CR patterns, and void fraction of coolant. Anisotropy of migration area, M_z^2/M^2 , was estimated from a series of measurements to understand the possible causes resulting in the difference of the CR-worth between experiment and calculation.

Calculations were mostly done by the absorption area method (A.A. method), which was employed in the design calculation of the FUGEN CR's. The calculation of the CR-worth agreed with the experiments within $\pm 10\%$. The calculation tended to somewhat overestimate the worth in the 0% void core and underestimate it in the 100% void core. This tendency was greatly improved by taking the anisotropy of migration area M^2 into consideration. The A.A. method calculations were supported by the direct full-core diffusion calculations applying the logarithmic derivative conditions on the surface of the CR (L.D. method). The L.D. method predicted better flux shape near the control rods.

VI. ACKNOWLEDGMENTS

Measurement was assisted by DCA staffs and Mr. Y. Kawamura of the Univ. of Kushu. The authors are indebted to Mr. H. Sakata and Mr. H. Kikuchi for valuable discussions and suggestions.

VII. REFERENCE

1. H. HURWITZ, Jr and G.M.ROE, J. Nucl. Energy, 2,85 (1955).
2. P. GREEBLER, Nucl. Sci. Eng., 3, 445 (1958).
3. S. PEARLSTEIN, Nucl. Sci. Eng., 4, 322 (1958).
4. R.W. DEUTSCH, Nucl. Sci. Eng., 5, 150 (1959).
5. Y. MIYAWAKI and H. KATO, PNC-report N941 74-72, presented at IAEA Panel on Plutonium Utilization in Thermal Power Reactor, 25-29 Nov. 1974, Karlsruhe.
6. M. J. BRINKWORTH and J.A. GRIFFITHS, AEEW-R480, (1966).
7. R. ALPIAR, AEEW-R135, (1964).
8. M. J. BRINKWORTH, AEEW-R631, (1969).
9. G. R. KEEPIN, T.F. WIMETT, and R.K. ZEIGLER, Phys. Rev. 107(4), 1044(1957).
10. S. BERNSTEIN, W.M. PRESTON, G.WOLFE, and R.E. SLATTERY, Phys. Rev. 71(9), 573(1947).
11. W. K. ERGEN, ANP-59, (1951).
12. A.M. WEINGERG, E.P. WINGNER, and WILLAMSON, CP-146 (1944).
13. C.R. RICHEY and T.J. OAKES, Nucl. Sci.Eng., 47, 40 (1972).
14. M. UEDA, J. Nucl. Sci. Technol., 12, 31 (1975).

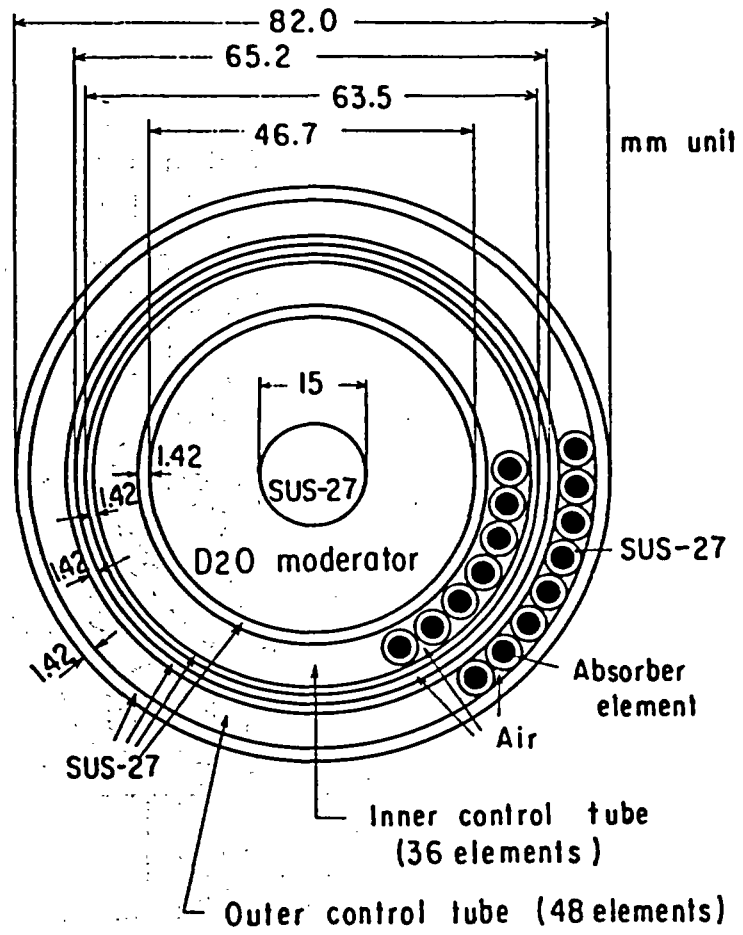


Fig. 1. Cross-sectional view of control rod.

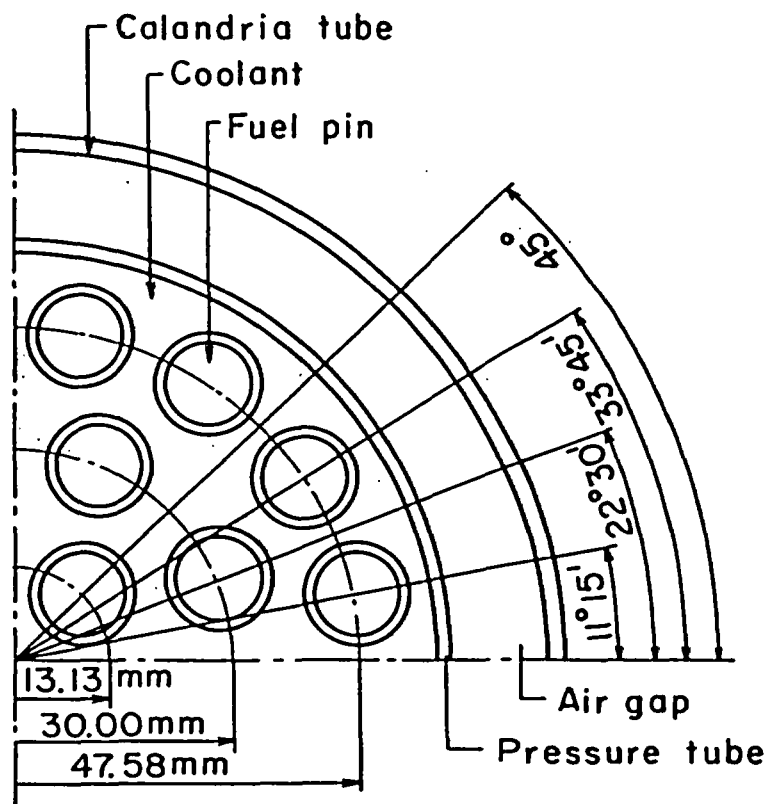


Fig.2. Quadrant cross section of fuel cluster.

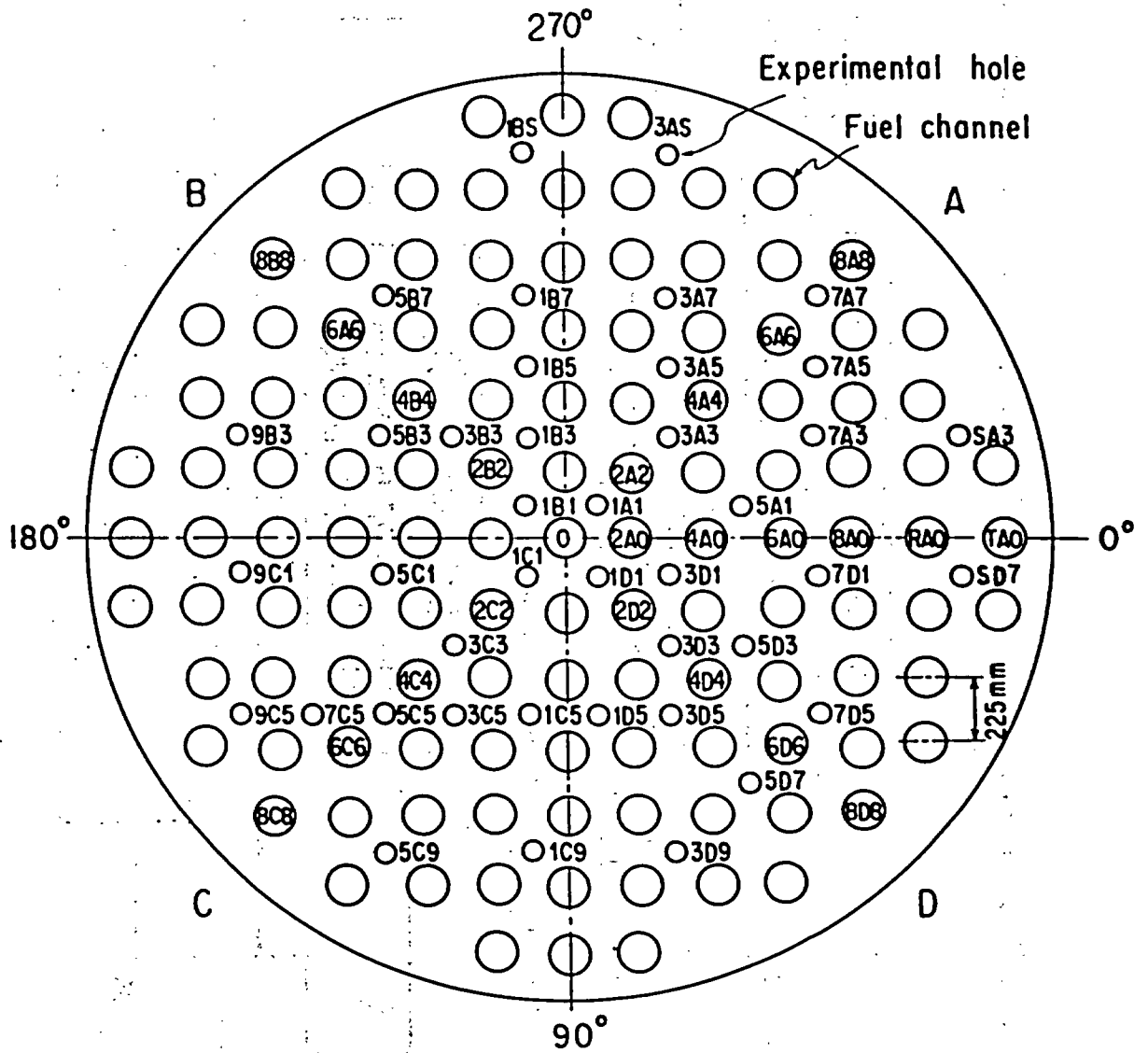


Fig. 3. Plan view of reactor core.

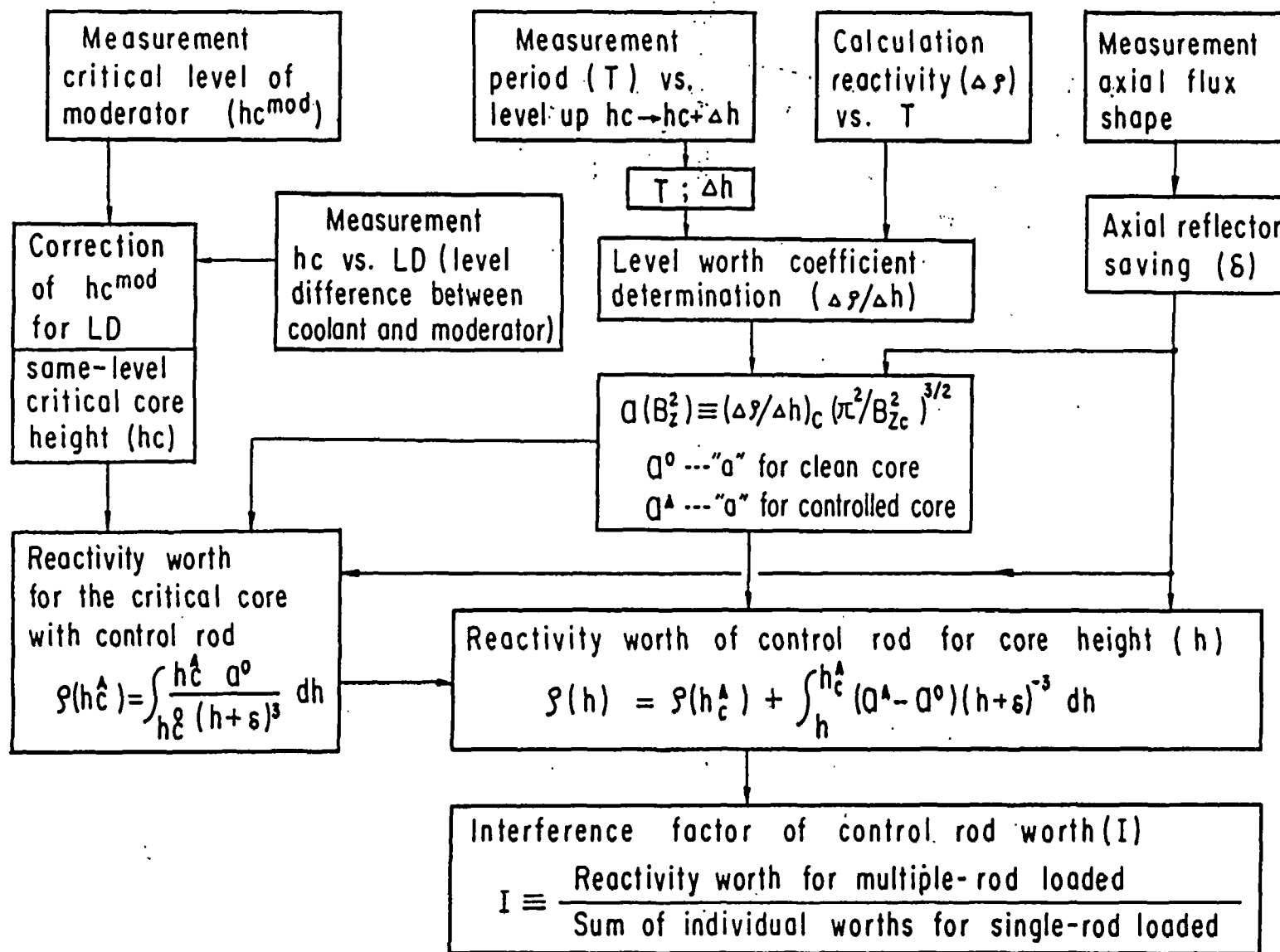


Fig 4. Experimental procedure.

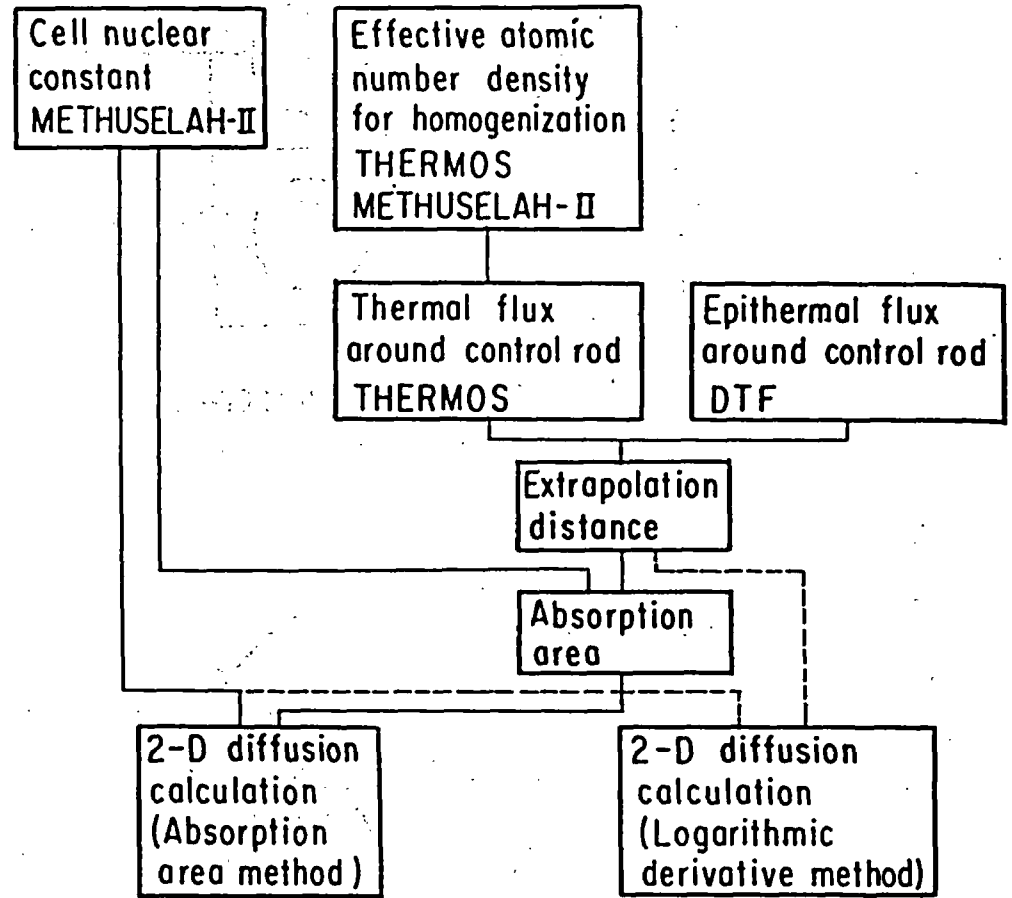
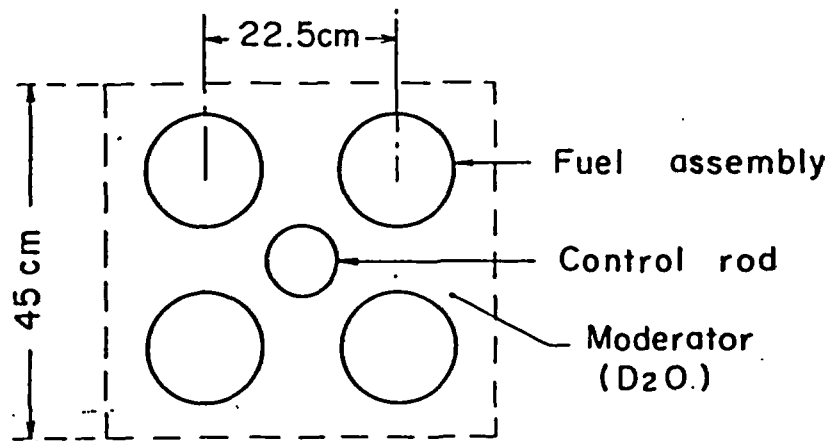
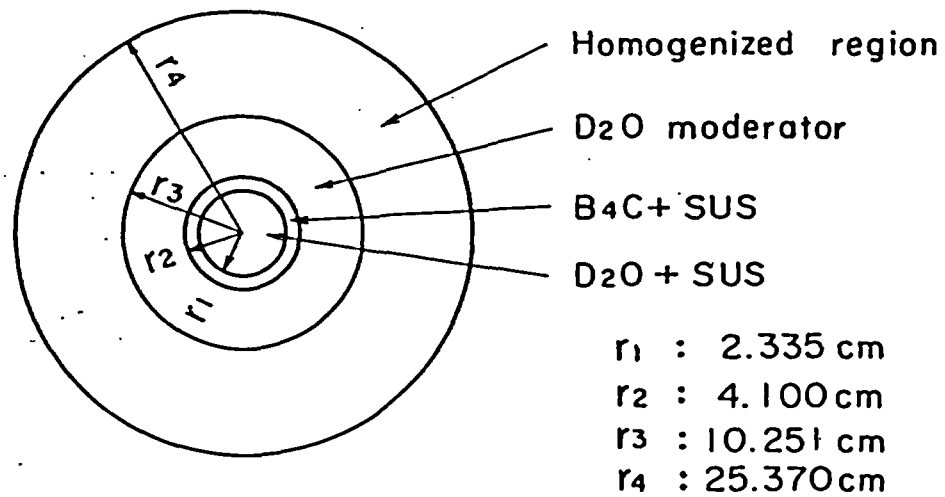


Fig. 5. Flow diagram of calculation.



(A) Controlled super-cell



(B) Cylindricalized controlled super-cell

Fig.6. Cylindricalization of controlled super-cell.

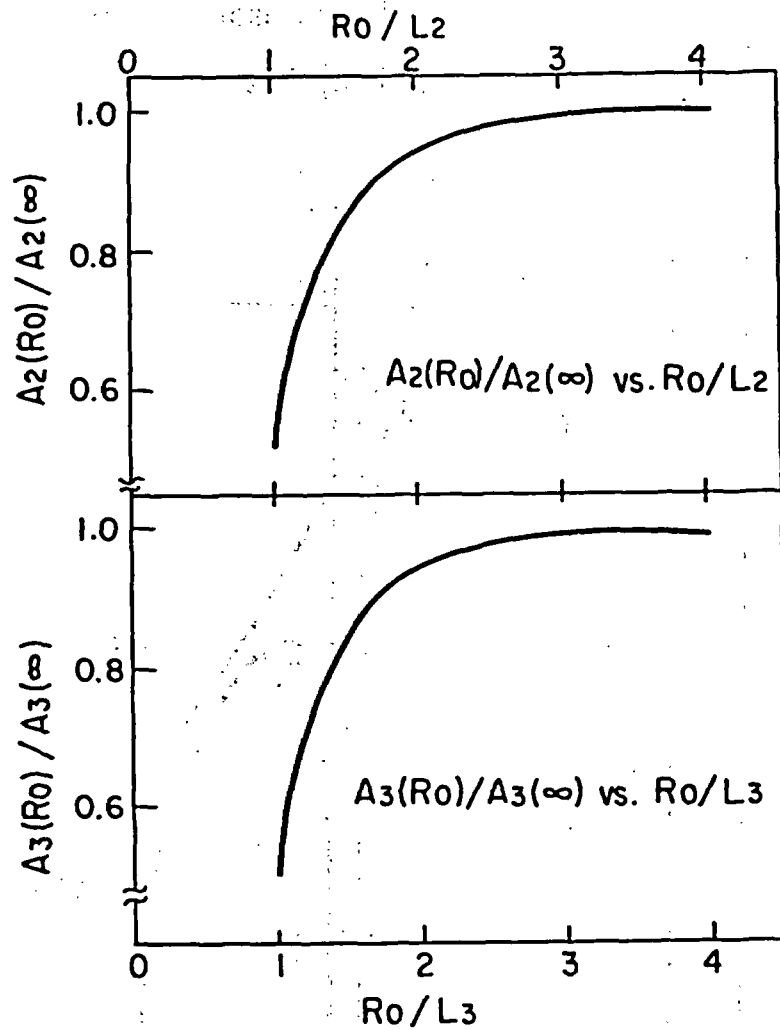


Fig.7. Relative Variations of Absorption Areas

Solid lines correspond to the absorption areas for 0 %-void "Controlled super-cell"

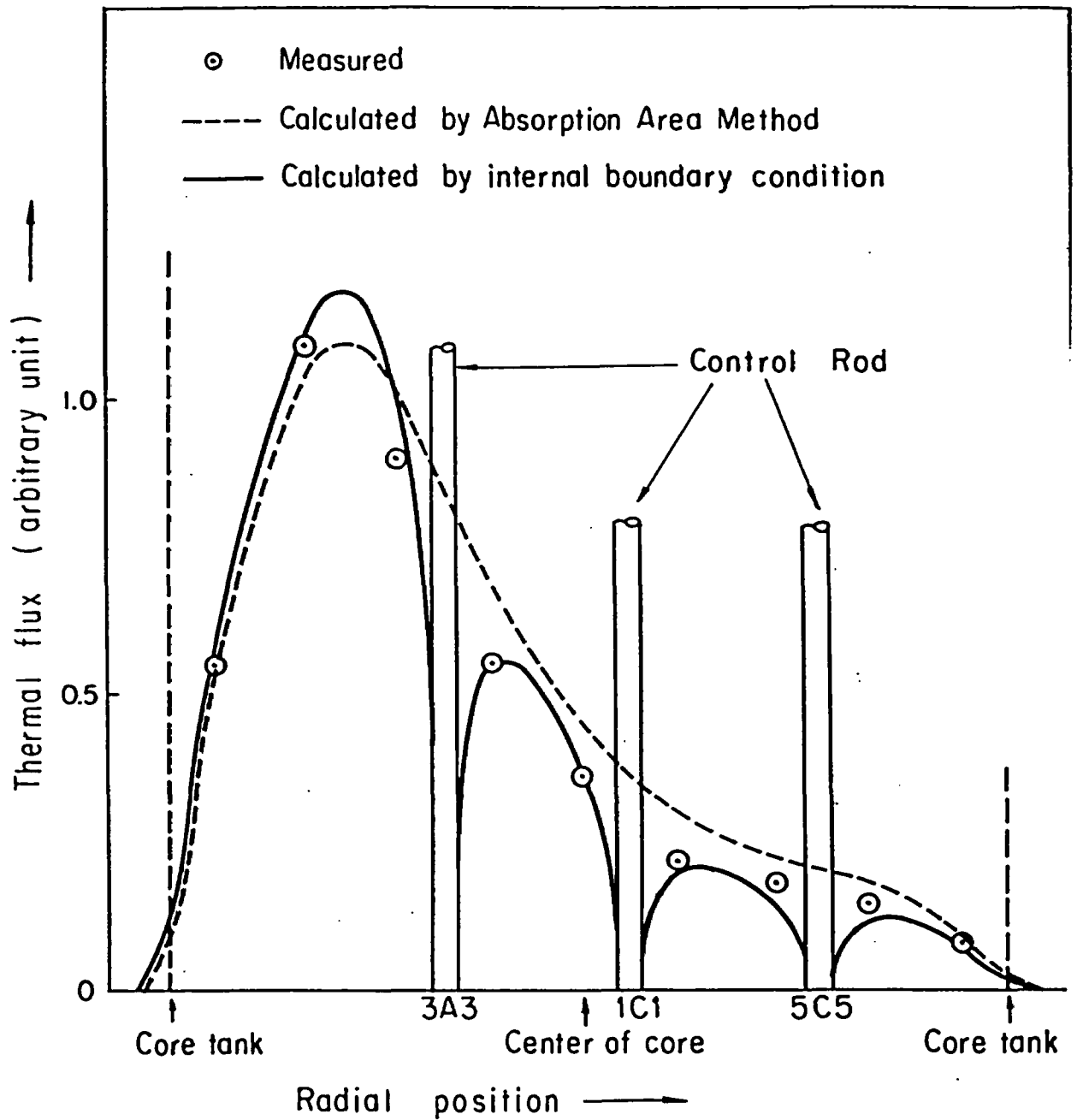


Fig.8. Correlation of measured and calculated thermal flux shapes in the 0%-void core with 9-control rod fully inserted. (see TABLE , Core No.23)

TABLE I. DCA Lattice Data

Region	Descriptions																																														
Cluster	<p>Diam : 11.68cm, total number : 121 Pellet : UO_2, 10.357g/cm^3, 1.48cm diam. 1.204wt% enriched Clad : Aluminum (JIS A2T1), 1.673cm outer diam, 0.85cm thick Radii of fuel rings : 13.13, 30.00, and 47.58mm Coolant : H_2O, $H_2O + D_2O + H_3BO_3$ (mixtures), 99.50mol/ o D_2O, or air</p> <table border="1" style="margin-left: auto; margin-right: auto;"> <thead> <tr> <th colspan="6">Ingredient and density of void-simulated coolant</th> </tr> <tr> <th rowspan="2">$\xi\Sigma_s$ equivalent void ratio (%)</th> <th colspan="4">Weight %</th> <th rowspan="2">density (g/cm^3)</th> </tr> <tr> <th>H_2O</th> <th>D_2O</th> <th>H_3BO_3</th> <th>air</th> </tr> </thead> <tbody> <tr> <td>0</td> <td>100</td> <td>0</td> <td>0</td> <td>0</td> <td>0.9981</td> </tr> <tr> <td>30</td> <td>63.2</td> <td>36.8</td> <td>0.0092</td> <td>0</td> <td>1.036</td> </tr> <tr> <td>70</td> <td>18.1</td> <td>81.9</td> <td>0.0215</td> <td>0</td> <td>1.087</td> </tr> <tr> <td>86.7</td> <td>0.47</td> <td>99.53</td> <td>0</td> <td>0</td> <td>1.1048</td> </tr> <tr> <td>100</td> <td>0</td> <td>0</td> <td>0</td> <td>100</td> <td>0</td> </tr> </tbody> </table>	Ingredient and density of void-simulated coolant						$\xi\Sigma_s$ equivalent void ratio (%)	Weight %				density (g/cm^3)	H_2O	D_2O	H_3BO_3	air	0	100	0	0	0	0.9981	30	63.2	36.8	0.0092	0	1.036	70	18.1	81.9	0.0215	0	1.087	86.7	0.47	99.53	0	0	1.1048	100	0	0	0	100	0
Ingredient and density of void-simulated coolant																																															
$\xi\Sigma_s$ equivalent void ratio (%)	Weight %				density (g/cm^3)																																										
	H_2O	D_2O	H_3BO_3	air																																											
0	100	0	0	0	0.9981																																										
30	63.2	36.8	0.0092	0	1.036																																										
70	18.1	81.9	0.0215	0	1.087																																										
86.7	0.47	99.53	0	0	1.1048																																										
100	0	0	0	100	0																																										
Pressure tube	12.08cm outer diam, 0.2cm thick, aluminum (JIS A2T1)																																														
Air gap	13.25cm outer diam																																														
Calandria tube	13.65cm outer diam, 0.2cm thick, aluminum (JIS A2T1)																																														
Moderator	99.50 mol/o D_2O , $1.1048\text{g/cm}^3(20^\circ\text{C})$																																														
Lattice	Square arrays spaced at 22.5cm																																														
Core tank	300.5cm inner diam, 1.0cm thick, aluminum (JIS A2P1)																																														
Grid plates	Upper and lower, aluminum (JIS A2P1)																																														
Lower absorber plate	$B_4C + Al$ (thermally black)																																														
Temperature	Room temperature 20°C																																														

TABLE II. Axial Reflector Saving and a-Value

Coolant Void Ratio (%) of core	Axial Reflector Saving (cm)	a-Value $\times 10^6$ (ϕ .cm ²)	Range of Axial Buckling B_z^2 (m ⁻²) Measured
0	10.5	39.6	4 - 9
30	11.2	39.8	5.4 - 8.2
70	11.8	$53.2 - 0.788 \times 10^4 B_z^2 (h_c^A)$	4.7 - 7.6
86.7	12.4 ^a	59.1	7.1 - 7.4
100	13.8	$78.0 - 1.31 \times 10^4 B_z^2 (h_c^A)$	2.4 - 6.2

a Estimated graphically

TABLE III. Critical Buckling and Reactivity Worth of Control Rod

Core No.	No. of C.R.	Coolant Void Ratio (%) Position of C.R.(Control Rod)Loaded	Critical Axial Buckling, $B_z^2(m^{-2})$					Worth (\$) for $B_z^2=6.11(m^{-2})$				
			0	30	70	86.7	100	0	30	70	86.7	100
1	0		8.67	8.37	7.54	7.30	6.11	1.51				
2	1	1D1	7.92	7.65	6.83	6.65	5.49	1.51	1.45	1.69	2.07	2.23
3	1	3D1	8.02				5.59	1.29				1.89
4	1	3D3	8.12				5.67	1.08				1.60
5	1	1D5	8.22	7.94	7.12	6.92	5.73	0.90	0.85	1.00	1.28	1.37
6	1	3D5	8.27				5.78	0.79				1.19
7	1	5D7	8.50	8.20	7.38		5.95	0.34	0.33	0.40		0.58
8	2	1B1+1D1	7.32	7.06	6.26		5.00	2.70	2.64	3.07		4.05
9	2	3B3+3D3	7.43				5.08	2.48				3.73
10	2	1B5+1D5	7.59	7.33	6.52	6.35	5.21	2.15	2.09	2.44	2.99	3.24
11	2	5B7+5D7	8.29	8.01	7.19		5.77	0.76	0.71	0.84		1.23
12	2	1B1+1C1	7.44				5.08	2.46				3.74
13	2	1B3+1C1	7.35				5.02	2.63				3.97
14	4	1A1+1B1+1C1+1D1	6.77	6.51	5.71		4.49	3.80	3.74	4.44		5.92
15	4	5A1+1B5+5C5+1D5	6.19	6.01	5.26		4.12	4.85	4.76	5.54		7.34
16	4	3A3+1B3+1C1+3D1	6.42				4.22	4.51				6.97
17	4	3A3+5B3+5C5+3D5	6.60	6.33	5.53		4.37	4.15	4.11	4.86		6.40
18	5	3A3 +5B3 +1C1 +3D5 +5C5	5.84	5.58	4.81		3.75	5.67	5.61	6.68		8.77
19	7	1B3+5B3+3D1+1C1+5C1+3D5+1C5	5.36				3.28	6.62				10.59
20	8	1B3+5B3+3D1+1C1+5C1+3D5+1C5+5C5	5.32				3.23	6.70				10.79
21	8	3A3+1B3+5B3 +1C1+5C1+3D5+1C5+5C5	4.91				2.91	7.52				12.05
22	8	3A3+1B3+5B3+3D1 +5C1+3D5+1C5+5C5	4.49				2.59	8.37				13.33
23	9	3A3+1B3+5B3+3D1+1C1+5C1+3D5+1C5+5C5	4.30				2.38	8.75				14.16

TABLE IV. Activation Traverse Data

Core Number	Position of Control Rod	Coolant Void (%)	Reaction of Sample	Relative Activation Rate at the Center of Fuel Cluster									Remarks (statistical error etc.)
				8C8	6C6	4C4	2C2	0	2A2	4A4	6A6	8A8	
1	No control rod	0.100	Bare Cu (2mm diam, wire)	0.25	0.52	0.75	0.93	1.00	0.93	0.75	0.52	0.25	Radial reflector saving:15cm
9	3B3+3D3	100	"	0.47	0.89	1.19	1.29	1.29	1.25	1.13	0.82	0.45	~ 0.5%
	3A3+3C3	100	"	0.36	0.64	0.66	0.87	1.29	0.86	0.65	0.62	0.33	~ 0.5%
18	5B3, -, 3A3 -, 1C1, - 5C5, -, 3D5	100	"	0.37	0.52	0.79	0.93	1.11	1.20	1.15	1.18	0.63	~ 0.5%
22	5B3, 1B3, 3A3 5C1, -, 3D1	0	"	0.15	0.24	0.34	0.59	0.77	0.79	1.15	1.27	0.65	~ 0.7%
	5C5, 1C5, 3D5	100	"	0.24	0.31	0.41	0.69	0.85	0.82	1.07	1.21	0.74	~ 0.5%
23	5B3, 1B3, 3A3 5C1, 1C1, 3D1	0	"	0.090	0.160	0.205	0.25	0.42	0.64	1.05	1.25	0.63	~ 0.7%
	5C5, 1C5, 3D5	100	"	0.185	0.248	0.290	0.34	0.51	0.72	1.07	1.24	0.77	~ 0.5%

TABLE V. Control Rod Worths

Core No.	No. of C.R.	Coolant Void Ratio (%)	Experimental Results (\$)	Calculated Value (\$)	
				A.A. Method*	L.D. Method**
2	1	0	1.51	1.646	1.875
		100	2.23	2.069	2.394
5	1	0	0.90	0.971	0.986
10	2	0	2.15	2.313	-
15	4	0	4.85	5.247	5.578
20	8	0	6.70	7.379	-
21	8	0	7.52	8.324	-
22	8	0	8.37	9.272	9.658
23	9	0	8.75	9.790	10.058
		100	14.16	12.269	13.742

* Absorption area method

** Diffusion calculation with logarithmic derivative condition